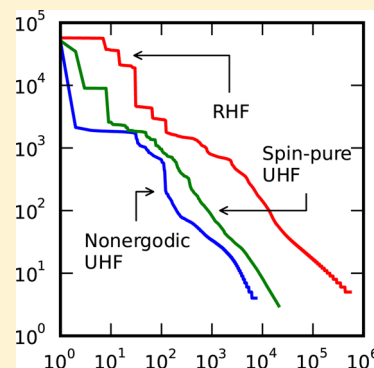


# Symmetry Breaking and Broken Ergodicity in Full Configuration Interaction Quantum Monte Carlo

Robert E. Thomas, Catherine Overy, George H. Booth, and Ali Alavi\*

The University Chemical Laboratory, University of Cambridge, Lensfield Road, Cambridge CB2 1EW, United Kingdom

**ABSTRACT:** The initiator full configuration interaction quantum Monte Carlo method (*i*-FCIQMC) is applied to the binding curve of  $N_2$  in Slater-determinant Hilbert spaces formed of both canonical restricted Hartree–Fock (RHF) and symmetry-broken unrestricted Hartree–Fock (UHF) orbitals. By explicit calculation, we demonstrate that the technique yields the same total energy for both types of orbital but that as the bond is stretched, FCI expansions expressed in unrestricted orbitals are substantially more compact than their restricted counterparts and more compact than those expressed in split-localized orbitals. These unrestricted Hilbert spaces, however, become nonergodic toward the dissociation limit, and the total wave function may be thought of as the sum of two weakly coupled, spin-impure, functions whose energies are nonetheless very close to the exact energy. In this limit, it is a challenge for *i*-FCIQMC to resolve a spin-pure wave function. The use of unrestricted natural orbitals is a promising remedy for this problem, as their expansions are more strongly weighted toward lower excitations of the reference, and they provide stronger coupling to higher excitations than do UHF orbitals.



## 1. INTRODUCTION

In dealing with strongly correlated electronic systems, symmetry breaking is a technique that is widely used to capture some electronic correlation beyond restricted Hartree–Fock (RHF) theory, while maintaining a relatively simple description of the electronic wave function. For example, the energy of a dissociating  $H_2$  molecule, which is the simplest prototype of a strongly correlated molecule, can be reasonably well described by a single Slater determinant (i.e., the unrestricted Hartree–Fock (UHF) wave function) formed out of spin-unrestricted Hartree–Fock orbitals, and in the dissociation limit of  $H_2 \rightarrow H + H$ , the UHF energy goes to the exact value of  $-1 E_h$ . “Spin unrestricted” means that the spatial orbitals ( $\phi_{i,\sigma}(\mathbf{r})$ ) associated with the two spin components ( $\sigma = \alpha, \beta$ ) are allowed to differ from each other (i.e.,  $\phi_{i,\alpha}(\mathbf{r}) \neq \phi_{i,\beta}(\mathbf{r})$ ), enabling some degree of spatial correlation to be introduced between an  $\alpha$ -electron and a  $\beta$ -electron into the UHF wave function. In Hartree–Fock theory, this symmetry breaking occurs spontaneously as the diatomic molecule is stretched, at the so-called the Coulson–Fischer (CF) point<sup>1</sup> and generally speaking results in the localization of the UHF orbitals on each nucleus (in contrast to RHF theory, where the molecular orbitals remain delocalized and can be labeled according to the irreducible representations of the point group of the molecule).

The UHF wave function is in general spin-contaminated, i.e., is not an eigenfunction of the  $\hat{S}^2$  operator, which for a nondegenerate state, the exact solution must be. Two observations are in order here. First, in the limit of infinite separation of the two hydrogen atoms, the corresponding ground-state becomes degenerate: the  $S = 0$  singlet state and the  $S = 1$  triplet state have the same energy in this limit. In such cases, it is obvious that the exact wave function need not be an

$\hat{S}^2$  eigenstate: any linear combination of the two energy-degenerate states is also an exact solution of the Hamiltonian, and if the two states in question have different values of  $S$ , the resulting linear combination cannot be an eigenfunction of  $\hat{S}^2$ . In this dissociation limit, therefore, the UHF wave function is able to constitute an exact solution of the  $H_2$  molecule despite not being a spin eigenstate.

Second, the full configuration interaction (FCI) energy, being a trace over the exact density matrix and the Hamiltonian, is invariant under orthonormal transformations of the underlying one-particle basis.<sup>2–5</sup> This statement, which arises from the mathematical properties of traces, is true for all systems, degenerate or not. The FCI wave function is a linear combination of the combinatorially large complete set of Slater determinants formed out of distributing  $N$  electrons in  $M$  spatial orbitals. Therefore it does not, in principle, matter whether one expands the FCI wave function in determinants formed out of restricted or unrestricted orbitals: both should yield the same exact total energy. However, the description of the FCI wave function will be different in the two approaches. For example, the degree to which the Hartree–Fock determinant is dominant may be significantly different, and this feature may be exploitable to our advantage.

Recently, full configuration interaction quantum Monte Carlo (*i*-FCIQMC) has been developed as a stochastic technique capable of yielding the full CI energy to within modest stochastic error bars, at a greatly reduced cost and scaling compared to conventional FCI.<sup>6,7</sup> Being a stochastic method, the underlying sparsity of the wave function is instrumental in determining the cost of the calculation, since a

Received: September 23, 2013

Published: March 19, 2014

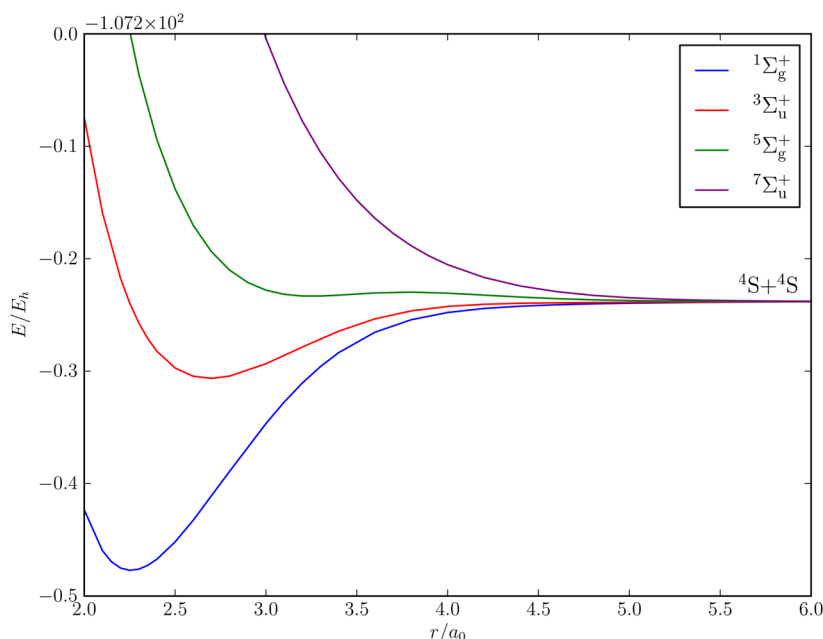


**Figure 1.** FCI binding curves for the ground state ( $1\Sigma_g^+$ ) and low-lying excited states, cast in a STO-3G basis.

sparse eigenvector can in general be more easily sampled than a dense one. It is, therefore, an interesting question to ask how the method compares when using symmetry-broken as opposed to canonical RHF orbitals. We should recover the same total energy in both cases, but because the representation of the underlying wave function is different, the computational cost of achieving FCI energies may be markedly different.

The electronic structures of the first-row diatomics have historically proven difficult to describe from first principles and are consequently excellent testing grounds for new ab initio methods.<sup>8–13</sup> In this study, we apply this simple adaptation—constructing the determinant space from a set of spin-unrestricted orbitals—and explore the consequences of so doing. Such orbitals have been used in the context of the auxiliary-field quantum Monte Carlo method with promising results.<sup>14–16</sup>

Many previous studies have shown that in a restricted basis, the FCI wave functions of the first-row homonuclear diatomics ( $C_2$ ,  $N_2$ ,  $O_2$ , and  $F_2$ ) become more multiconfigurational as their bonds are stretched.<sup>17,18</sup> To this end, the stretched geometries require more walkers and thus more computational effort to resolve than those at equilibrium. This trend, however, is reversed in the heteronuclear cases<sup>18</sup> and motivates the present discussion of unrestricted orbitals.

## 2. FCIQMC AND THE INITIATOR ADAPTATION

FCIQMC and *i*-FCIQMC have been expounded in detail in previous papers,<sup>6,7,19–21</sup> so we present only a brief summary here. *i*-FCIQMC yields coefficients  $\{C_i\}$  of a wave function as the (normalized) signed sum of walkers on each determinant  $|D_i\rangle$ . This is achieved by submitting the walkers to an iterative, three-step algorithm, characterized by “spawning”, “death”, and “annihilation” processes. *i*-FCIQMC differs from FCIQMC only in that in the former case, a walker may be spawned on to an unoccupied determinant only if the population on the parent determinant exceeds some threshold,  $n_a$ . Two independent measures, the projected energy,  $E_{\text{proj}}$ , and the “shift”,  $\mu$ , give the energy of the distribution. (Note: in previous papers,<sup>6,7,20,22</sup> we

referred to the shift with the symbol  $S$ . Here, because we want to avoid confusion with the spin  $S$ , we change notation to use  $\mu$ . This also reflects the fact that the shift can be considered as the chemical potential of the walkers in Hilbert space).

This initiator approach reduces to the original algorithm in both the limits of large walker number and reducing  $n_a$ , such that its results are systematically improvable. Typically, this is achieved by converging the energy with respect to increasing the total number of walkers,  $N_w$ , whereby we can determine a suitable walker population to ensure that any systematic error is negligible.<sup>7,20,22</sup> We therefore proceed with the use of *i*-FCIQMC for the remainder of this paper.

Symmetry has been successfully exploited in FCIQMC to reduce both the size and connectivity of the space.<sup>6,17</sup> Since the Hamiltonian operator belongs to the totally symmetric irreducible representation,  $\Gamma_1$ , of any point group, the Hamiltonian matrix elements,  $\langle D_i | \hat{H} | D_j \rangle$ , will be zero unless

$$\Gamma_{D_i} \otimes \Gamma_{D_j} \ni \Gamma_1 \quad (1)$$

Much of this symmetry can be maintained in the spawning step, thereby avoiding the evaluation of zero matrix elements. This is lost when using symmetry-broken orbitals, which give rise to a more connected Slater-determinant network and would perhaps necessitate a smaller time step,  $\delta\tau$ . This can be understood by considering the probability of spawning a walker on determinant  $|D_j\rangle$  from a parent on a coupled determinant  $|D_i\rangle$ ,<sup>6</sup>

$$p_s = \frac{\delta\tau |\langle D_i | \hat{H} | D_j \rangle|}{P_{\text{gen}}(D_j | D_i)} \quad (2)$$

$P_{\text{gen}}$  is the normalized probability of selecting determinant  $|D_j\rangle$  from  $|D_i\rangle$  and will decrease if the space is more connected, for example, as a result of a reduction in symmetry on going from an RHF to a UHF basis. We might, therefore, expect to require a reduction in  $\delta\tau$  in order to maintain  $p_s$ .

Additionally, in the case of systems with equal numbers of  $\alpha$  and  $\beta$  electrons, time-reversal symmetry can be applied to RHF

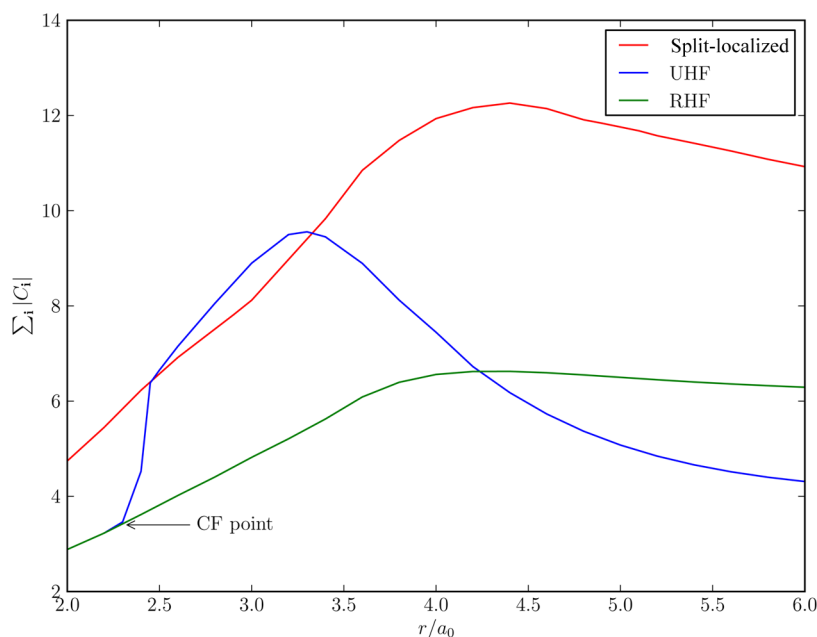


**Figure 2.** Sums of the absolute coefficients,  $\sum_i |C_i|$ , as a function of bond length for RHF, UHF, and split-localized STO-3G FCI expansions. The unrestricted orbitals provide a more compact basis as the bond is stretched away from equilibrium. Either CASSCF approach for the split-localized orbitals (see text) yields the same total compactness for the FCI solution. The CF point is illustrated.

basis sets, leading to a further reduction in the number of degrees of freedom and also, potentially, allowing a larger time step.<sup>17</sup> It is, therefore, not at all obvious that a UHF approach can be advantageous in FCIQMC, since such savings will be lost upon discarding the orbital symmetry labeling.

### 3. RESULTS AND DISCUSSION

#### 3.1. A Motivating Case: The STO-3G Nitrogen Dimer.

We begin with an analysis of the FCI expansions for  $N_2$  in both RHF and UHF STO-3G bases.<sup>23</sup> This minimal representation allows exact results to be readily obtained, and the FCI binding curves of the ground state,  $^1\Sigma_g^+$ , and low-lying excited states,  $^3\Sigma_u^+$ ,  $^5\Sigma_g^+$ , and  $^7\Sigma_u^+$ , which lead to a 4-fold degenerate ground state in the  $^4S + ^4S$  dissociation limit, are illustrated in Figure 1. A significant part of the challenge of describing the stretched molecule arises from the near degeneracy of these four states.

We explicitly verified that both bases provide the same total energy for a given geometry. An analysis of the relative compactness of the expansions for the  $^1\Sigma_g^+$  state, however, reveals them to be markedly different. Figure 2 plots the total sum of the absolute CI coefficients,  $\sum_i |C_i|$ , across the binding curve for both bases. (The wave function is normalized so that  $\sum_i |C_i|^2 = 1$ ). This quantity is proportional to the number of walkers required for an  $i$ -FCIQMC calculation to exactly distribute the walkers according to the ground-state eigenvector. This implies that the UHF expansion becomes significantly more compact than its restricted counterpart without any loss of spin purity as the bond is stretched, which bodes well for studies in larger bases (Figure 2).

This compactness may be rationalized as being afforded by the localization of UHF orbitals toward the stretched limit. Consider, for example, a determinant in which there are  $N_1$  electrons on nucleus 1 and  $N_2$  electrons on nucleus 2, with  $N_1 + N_2 = N$ . There are  $\sum_{N_1} \binom{M}{N_1} \binom{M}{N - N_1} = \binom{2M}{N}$  determinants overall, which is the total size of the Hilbert space, of which the

neutral configurations constitute  $\left(\frac{M}{N/2}\right)^2$  ( $M$  being the number of spatial orbitals). The fraction of determinants which are neutral is therefore  $\left(\frac{M}{N/2}\right)^2 / \binom{2M}{N}$ , this fraction decreasing as  $O(N^{-1})$  for increasing  $N$ . In a stretched diatomic, the accessible part of the Hilbert space consists of the determinants in which each atomic fragment is neutral, with determinants in which one or more electrons have been transferred from one nucleus to the other being unfavorable and suppressed in the ground-state expansion. This constraint of having neutral fragments implies an  $O(N)$  reduction in the Hilbert space and thus contributes to the observed sparseness of the ground-state wave function in the UHF basis.

Figure 2 also illustrates the same compactness metric for another localized, symmetry-broken basis readily available from Molpro:<sup>24</sup> split-localized orbitals.<sup>25</sup> These are obtained by first calculating approximate natural orbitals to define a strongly occupied and a strongly unoccupied set of orbitals. These two sets are then localized separately (our localization procedure here is the Pipek–Mezey scheme,<sup>26</sup> but others<sup>27</sup> yield similar results) to give the new orbitals. We obtain the natural orbitals from both 10-electron, 8-active orbital CASSCF<sup>28,29</sup> (which recovers the FCI energy) and 6-electron, 6-active orbital CASSCF calculations. In either approach, this basis induces no such sparsity in the FCI, as the orbitals remain centered on both atomic sites rather than just one, as is the case for UHF orbitals. We therefore proceed with the use of the latter.

**3.2. Moving to a Larger Basis.** The observations in the STO-3G basis suggest that UHF orbitals should be preferred toward the dissociation limit. We return to that proposition later, but we first turn to the intermediate regime. Much of the interesting chemistry and physics of the diatomics takes place in this regime, where there is competition between correlation effects and one-electron energetics. Our initial focus, therefore, is ascertaining where along the binding curve the UHF

**Table 1.** Frozen-Core cc-pVDZ *i*-FCIQMC Energies of the N<sub>2</sub> Molecule (<sup>1</sup>Σ<sub>g</sub><sup>+</sup>) at a Number of Different Bond Lengths, Alongside the Corresponding FCI Results of Chan et al. (ref 37)<sup>a</sup>

$r/a_0$	$E_{\text{FCI}}$	$\langle E_{\text{proj,RHF}} \rangle_\tau$	$\langle \mu_{\text{RHF}} \rangle_\tau$	$\langle E_{\text{proj,UHF}} \rangle_\tau$	$\langle \mu_{\text{UHF}} \rangle_\tau$	$N_{\text{w,RHF}}/10^6$	$N_{\text{w,UHF}}/10^6$
2.118	−109.278339	−109.27833(4)	−109.2782(2)	−109.27825(4)	−109.2779(2)	4.652	4.577
2.400	−109.238397	−109.2383(1)	−109.2381(2)	−109.2383(1)	−109.2383(2)	5.699	13.479
2.700	−109.160305	−109.16030(6)	−109.1601(2)	−109.1603(1)	−109.1602(3)	6.772	16.560
3.000	−109.086209	−109.0861(1)	−109.0862(2)	−109.0858(4)	−109.0860(3)	8.148	16.580
3.600	−108.994906	−108.9944(4)	−108.9949(3)	−108.9945(1)	−108.9946(2)	11.671	7.456
4.200	−108.966950	−108.9667(3)	−108.9667(2)	−108.9659(4)	−108.9669(2)	19.389	2.983

<sup>a</sup>Simulations on the more multiconfigurational systems often exhibited a decrease in  $N_0$  once the shift was allowed to vary, meaning that  $\langle \mu \rangle_\tau$  becomes a somewhat better estimator than  $\langle E_{\text{proj}} \rangle_\tau$ . The number in brackets represents the error in the previous digit, obtained through a Flyvbjerg–Petersen blocking analysis<sup>39</sup> of  $E(\tau)$ .

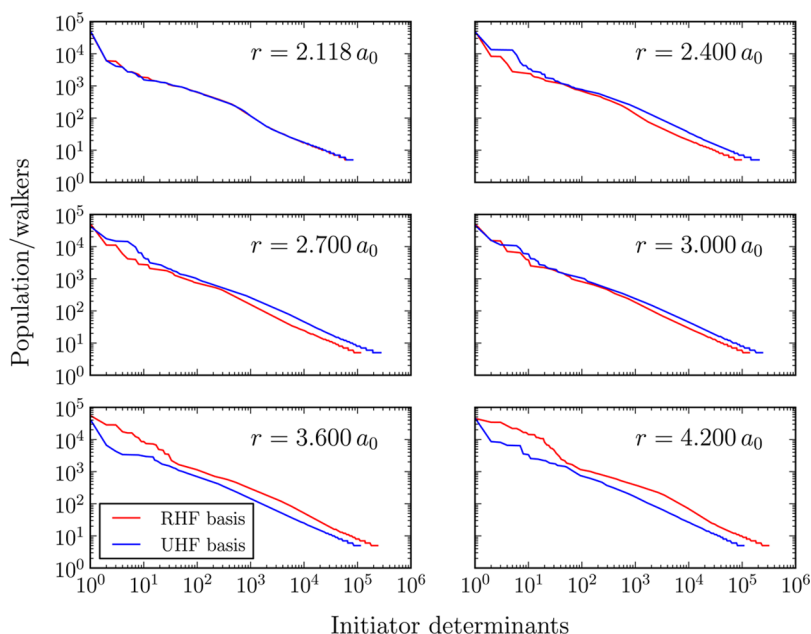


**Figure 3.** The absolute values of initiator populations, arranged in descending order, taken from equilibrated simulations of N<sub>2</sub> at different geometries with ~50 000 walkers on the HF determinant. At near equilibrium bond lengths, the UHF simulations require more walkers, but these wave functions become more compact as the bond is stretched. Conversely, the restricted wave functions are increasingly dense away from equilibrium.

becomes favorable for an *i*-FCIQMC simulation, and we take the (<sup>1</sup>Σ<sub>g</sub><sup>+</sup>) state of N<sub>2</sub> as an archetypal example.

As the triple bond is stretched, it becomes highly multiconfigurational, and so a description across the binding curve has long provided a challenge for electronic structure theories.<sup>30–35</sup> In particular, we evaluate frozen-core energies at six geometries ( $r = 2.118, 2.400, 2.700, 3.000, 3.600$ , and  $4.200 a_0$ ) in Dunning cc-pVDZ basis sets,<sup>36</sup> for which FCI results are available.<sup>37</sup>

Our primary concern here is a comparison of the two approaches, so these solutions are found in the comparatively small Dunning cc-pVDZ basis sets,<sup>36</sup> rather than aiming for chemical accuracy, which would necessitate much larger basis sets and which have been previously reported.<sup>18</sup> Moreover, the core electrons,  $(1\sigma_g)^2(1\sigma_u^*)^2$ , are frozen. The RHF orbitals in this study were computed using Molpro,<sup>24</sup> while the unrestricted orbitals were obtained from QChem, wherein we allow the spatial symmetry of the molecular point group to be ignored.<sup>38</sup> The energies of these UHF determinants are consistent with those obtained by Chan et al.<sup>37</sup> We adopt the *i*-FCIQMC protocol with  $\delta\tau = 10^{-4}$  au and  $n_a = 3$ , beginning with a single walker on the HF determinant and fixing  $\mu = 0$ . In

this regime, the number of walkers,  $N_w$ , grows exponentially until it reaches a target value, whereupon we allow  $\mu$  to vary so as to keep the walker population constant. This target value of  $N_w$  was chosen as that at which the population on the Hartree–Fock determinant,  $N_0$ , is 50 000 walkers as suggested in the previous study, which has been found empirically to lead to negligible systematic initiator error for systems such as these.<sup>18</sup> This criterion was applied to both UHF and RHF calculations.

Once  $N_0(\tau)$  (the number of walkers on the Hartree–Fock determinant) and  $E_{\text{proj}}(\tau)$  have equilibrated in the variable-shift regime, we may begin to estimate  $\langle N_0 \rangle_\tau$  and  $\langle E_{\text{proj}} \rangle_\tau$  and continue the simulation until the statistical errors in those quantities have been satisfactorily reduced. We adopt the Flyvbjerg–Petersen blocking algorithm to obtain estimates of the serial correlation time and perform this separately for the numerator and denominator of the projected energy.<sup>18,39</sup> The errors presented in brackets throughout this work correspond to the uncertainty in the preceding digit and represent one standard deviation in the energy distribution.

It is interesting to note that the same value of the time step is satisfactory in both bases, and that if we allow the time step to vary dynamically so as to eradicate particle blooms, the same



value,  $O(10^{-4})$ , is achieved. The implication from eq 2 is that the off-diagonal Hamiltonian matrix elements must be smaller in the UHF basis than in the restricted basis. Indeed, an explicit examination of these elements in the smaller STO-3G systems reveals that both the mean and the maximal values of  $\langle D_i | \hat{H} | D_j \rangle$  are smaller when unrestricted orbitals are used.

This approach yields the results of Table 1, and further insight can be gleaned from Figure 3. These plots reveal that the unrestricted calculations require more walkers than the restricted close to equilibrium, but this trend is reversed as the bond is stretched, mirroring the behavior observed in the smaller basis. In particular, we observe a “shelf” of highly weighted determinants developing in the restricted basis, while the unrestricted wave function becomes more compact.

*i*-FCIQMC delivers (in either basis) energies in close agreement with benchmark results,<sup>37</sup> but it is worth noting the challenges which these systems present the method. First, it is observed that for the more multiconfigurational systems (in particular  $r = 3.6$  and  $4.2 a_0$ ) there is an initial decrease in  $N_0$  after the shift  $\mu$  is allowed to vary before the population eventually stabilizes. This has the effect that the projected energy relaxes rather more slowly than the shift, making the latter the better energy estimator in this case.

In the  $r = 4.2 a_0$  system in particular, this problem is exacerbated by the slow growth of a 6-fold excited determinant, which corresponds to inverting the spins of all 6 2p electrons in the UHF determinant. The presence of this determinant is unsurprising given the need to restore spin purity. Indeed, it was observed in the STO-3G basis, wherein its weight grows steadily as the bond is stretched, until it matches that of the Hartree–Fock determinant. Its slow growth, however, implies that it is only weakly coupled to the region of the wave function dominated by the Hartree–Fock determinant and suggests that the unrestricted Hilbert space becomes nonergodic toward the dissociation limit.

Before turning to a discussion of broken ergodicity, we note for completeness that the split-localized orbitals yield a much less compact expansion than the UHF orbitals in this larger basis: the  $r = 4.2 a_0$  problem, for example, requiring 36 million walkers for convergence. In this basis, in which the orbitals are obtained using a 10-electron, 8-active orbital CASSCF calculation (with 18 external orbitals), the Pipek–Mezey localization procedure preserves the two-site character of the occupied and low-energy virtual orbitals, localizing on single atoms only the higher virtuals. This implies that localization of these orbitals plays a crucial role in inducing sparsity in the FCI solution.

**3.3. Broken Ergodicity and the Dissociation Limit.** The slow growth of an important determinant in the last section points toward an interesting feature of the UHF Hilbert space as the bond is stretched, namely, that it ceases to be ergodic.

This effect is at its most pronounced in the dissociation limit, to which we now turn our attention. The RHF expansion in this limit (taken to be 5 times the equilibrium bond length)<sup>18</sup> is highly multiconfigurational, and the *i*-FCIQMC calculation requires in excess of 20 million walkers to resolve the energy.

By contrast, an *i*-FCIQMC calculation initialized on the UHF determinant in the unrestricted basis yields an energy in close agreement with previous studies,<sup>18</sup> as listed in Table 2, at a cost of only 350 000 walkers. This factor of  $\sim 60$  saving, however, comes at the cost of spin purity: the wave function given by this calculation has  $C_{\text{UHF}} > 0.9$ , and there is no apparent growth of the 6-fold excitation demanded by symmetry even after many

**Table 2. Frozen-Core *i*-FCIQMC Energies of the Stretched  $\text{N}_2$  Molecule in a UHF Dunning cc-pVDZ Basis<sup>36</sup> Initialized on Different Determinants<sup>a</sup>**

initial configuration	$\langle E \rangle_\tau$	$N_w/10^6$
$ D_{0,L}\rangle$	−108.95732(3)	0.350
$ D_{0,R}\rangle$	−108.9574(3)	0.801
$ D_{0,L}\rangle +  D_{0,R}\rangle$	−108.95738(4)	0.886

<sup>a</sup>The spin-contaminated expansions (those initialised on a single determinant) give accurate energies, comparable to the spin-pure expansion, and all require fewer walkers than the corresponding RHF expansion, for which  $N_w = 22.765 \times 10^6$ .

hundreds of units of imaginary time. Likewise, initializing an *i*-FCIQMC calculation on the determinant with the 6 2p electrons flipped provides a good total energy and another (different) spin-contaminated wave function.

In this limit, therefore, one may consider the wave function to be the sum of two weakly coupled pockets, which we designate the “left-hand” and “right-hand” regions of the space,  $\Psi_L$  and  $\Psi_R$ . That is, we may write the total wave function as

$$\Psi = \frac{1}{\sqrt{2}}(\Psi_L + \Psi_R) \quad (3)$$

with  $\langle \Psi_L | \hat{H} | \Psi_R \rangle \rightarrow 0$  in the limit  $r \rightarrow \infty$ . The UHF determinant,  $|D_{0,L}\rangle$ , is the dominant determinant in  $\Psi_L$ , and the determinant with the spins of the 6 2p electrons inverted,  $|D_{0,R}\rangle$ , is dominant in  $\Psi_R$ .

This effect is illustrated explicitly for the system at  $6.0 a_0$  cast in a STO-3G basis<sup>24</sup> in Figure 4. The FCIQMC calculation is initialized with a single walker placed on the UHF determinant, and the population initially grows only on the doubly excited determinants, with very little exploration of the higher space. Thus,  $\Psi_L$  alone is explored initially and provides, on its own, a very good total energy. It is only after very many iterations that the right-hand pocket,  $\Psi_R$ , is explored, and the spin-pure eigenvector emerges.

Explicit examination of the Hamiltonian reveals the nature of the ergodic bottleneck. There exist only 150 coupling paths between  $|D_{0,L}\rangle$  and  $|D_{0,R}\rangle$  via two intermediate determinants, entailing the traversing of an energy barrier whose mean height is  $1.0015 E_h$ . Moreover, the values of the relevant matrix elements  $\langle D_i | \hat{H} | D_j \rangle$  are found to be significantly less than the mean value of a (nonzero) off-diagonal element, accounting for the very weak coupling between the two pockets.

A spin-pure wave function can, however, be converged upon by initializing the calculation with walkers on both  $|D_{0,L}\rangle$  and  $|D_{0,R}\rangle$ . This modification provides next to no improvement in the energy, as is clear from Figure 2, but does provide an FCI expansion containing comparable contributions from the dominant determinants. This eigenfunction, while requiring more walkers than the sampling of  $\Psi_L$  alone by a little more than a factor of  $\sim 2.5$ , still represents a walker saving by a factor of  $\sim 2.5$  over the RHF expansion.

**3.4. Other Diatomics.** The other homonuclear diatomics in this series,  $\text{C}_2$ ,  $\text{O}_2$ , and  $\text{F}_2$ , exhibit very similar behavior in their dissociation limits. Figure 3 presents the energies obtained for these stretched dimers from both RHF and UHF expansions. “Stretched” is taken, as before, to be 5 times the equilibrium bond lengths given by Huber and Herzberg.<sup>18,40</sup>

Here, again, both expansions yield energies in close agreement with previous results.<sup>18</sup> Once again, however, it is clear that very significant savings achieved by the UHF basis for

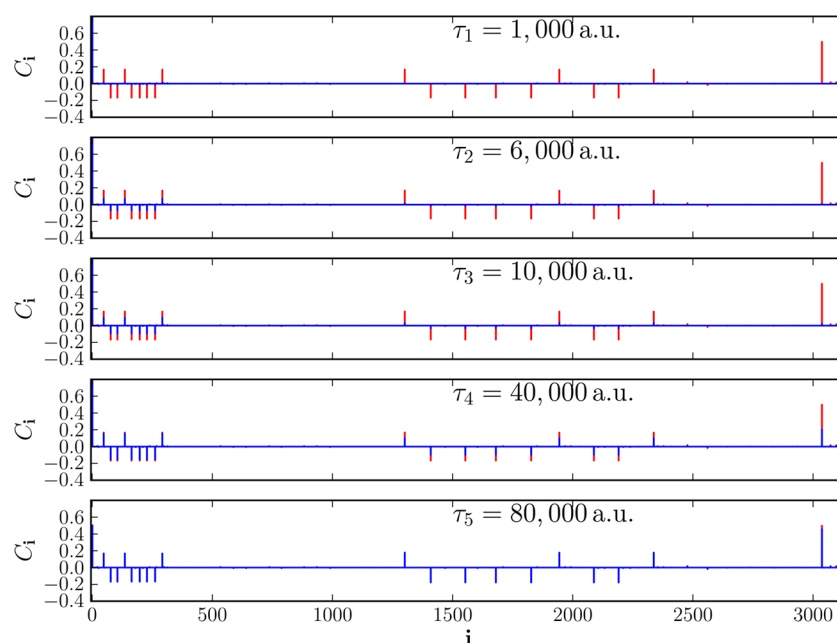


**Figure 4.** Imaginary-time evolution of the FCIQMC wave function initialized on the UHF determinant compared to the exact function for  $N_2$  with  $r = 6.0 a_0$  in a STO-3G UHF basis. The “left-hand” pocket,  $\Psi_L$ , is initially explored, and it is only much later that we observe substantial walker populations in the “right-hand” pocket,  $\Psi_R$ .

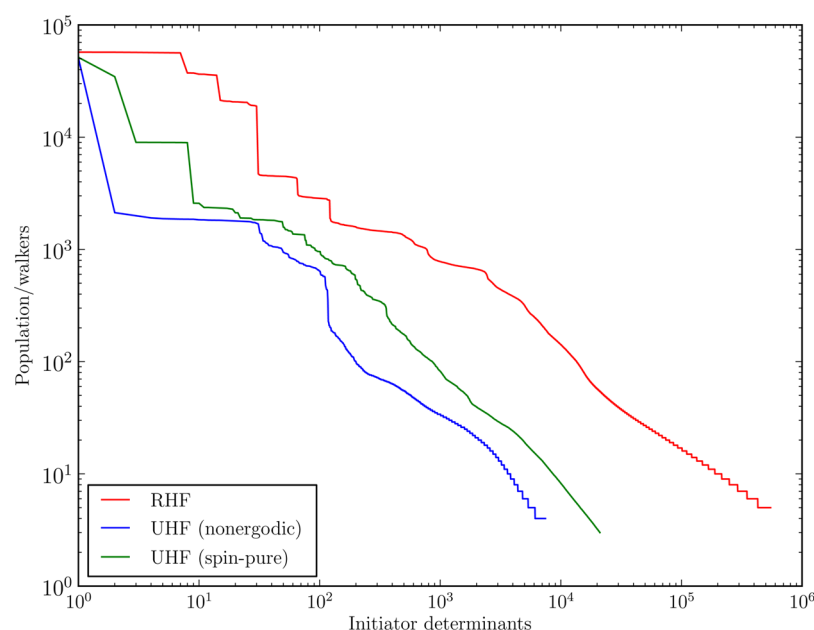


**Figure 5.** The absolute values of initiator populations, arranged in descending order, taken from equilibrated simulations of stretched ( $r = 5r_e = 10.59 a_0$ )  $N_2$  with  $\sim 50\,000$  walkers on the HF determinant. The spin-pure UHF expansion, while being less compact than the spin-contaminated wave function, is still significantly more sparse than the RHF expansion.

**Table 3. Frozen-Core FCIQMC Energies of the Stretched First-Row Homonuclear Diatomics in RHF and UHF Bases, Given by Both the Projected Energy,  $E_{\text{proj}}$ , and the Shift,  $\mu^a$**

system	$\langle E_{\text{proj,RHF}} \rangle_\tau$	$\langle \mu_{\text{RHF}} \rangle_\tau$	$\langle E_{\text{proj,UHF}} \rangle_\tau$	$\langle \mu_{\text{UHF}} \rangle_\tau$	$N_{w,\text{RHF}}/10^6$	$N_{w,\text{UHF}}/10^6$
$C_2$	−75.5210(3)	−75.5212(1)	−75.5213(1)	−75.5213(2)	8.281	1.116
$O_2$	−149.8204(4)	−149.8203(3)	−149.8209(4)	−149.8213(2)	16.527	10.807
$F_2$	−199.0556(4)	−199.0555(3)	−199.05550(5)	−199.0556(4)	5.847	0.653

<sup>a</sup>The bond lengths were taken to be 5 times the equilibrium lengths given by Huber and Herzberg,<sup>40</sup> and close agreement is achieved with the values previously obtained.<sup>18</sup> The number in brackets represents the error in the previous digit, obtained through a Flyvbjerg–Petersen blocking analysis<sup>39</sup> of  $E(\tau)$ . A Dunning cc-pVDZ basis set<sup>36</sup> was used in each case. The final two columns give the number of walkers required such that 50 000 reside on the reference determinant in both bases and were obtained by blocking  $N_w$  over the course of the calculations.

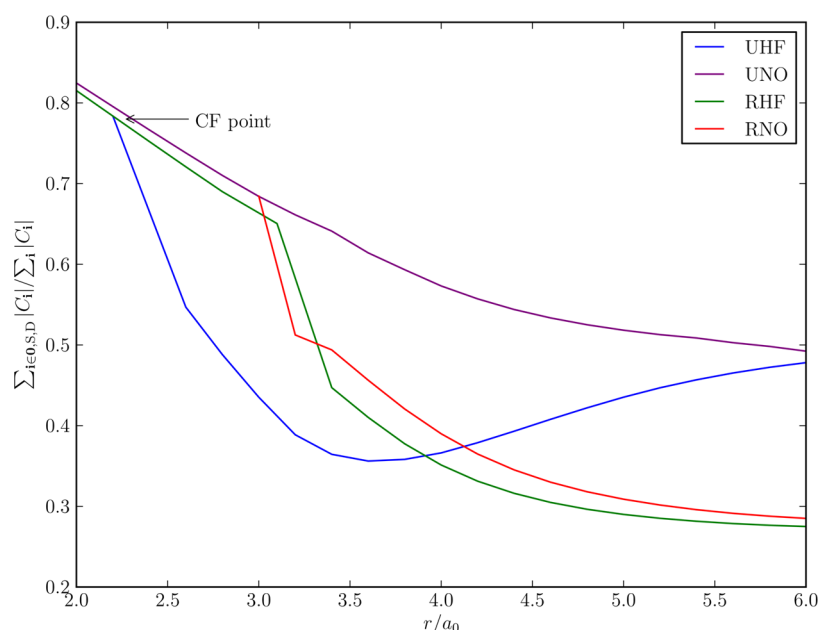


**Figure 6.** Fraction of the total wave function contained within the reference, singles, and doubles as a function of bond length for RHF, UHF, and UNO STO-3G FCI expansions. The UNO basis allows for a wave function which is more strongly weighted toward these low excitations, making for easier sampling. For completeness, the same fraction is plotted for the RNOs which do not exhibit the same behavior.

$C_2$  and  $F_2$  are at least partly the result of broken ergodicity, as both leading coefficients are around 0.9. The savings observed for  $O_2$ , whose leading coefficient is around 0.5, are a truer representation of the compactness achieved by a spin-pure UHF expansion. That broken ergodicity is not so significant a factor in this molecule can be rationalized, as we would expect  $|D_{0,R}\rangle$  to be only a double excitation of  $|D_{0,L}\rangle$  in this case, making them far closer in Hilbert space than was the case for  $N_2$ .

**3.5. A Possible Remedy: STO-3G Redux.** While the ergodicity problem can, in principle, be resolved by initializing a calculation with walkers in all the ergodic pockets, the requirement to know anything a priori about the wave function runs counter to the goal of achieving a black-box method. Moreover, presupposing the dominant determinants of each pocket will be less and less intuitively appealing for more complicated systems and so is unlikely to present a general way forward toward spin-pure wave functions. What is required, therefore, is a basis which preserves the compactness of the UHF basis, but which more heavily weights the lower excitations of the reference determinant and thus makes for easier sampling.

In the small STO-3G basis which motivated the original discussion, we can obtain unrestricted natural orbitals (UNOs) as the eigenfunctions of the exact one-body reduced density matrix,<sup>41–43</sup> and this new basis exhibits a number of desirable properties.

Across the binding curve, UNO expansions place a more sizable proportion of their total weights upon the reference, singles, and doubles, than do other bases. This trend is illustrated in Figure 6, which plots the ratio of the sum of the absolute coefficients in this subspace and the same sum over the whole space. For completeness, Figure 6 also illustrates the restricted natural orbitals (RNOs). While expansions in this basis do place higher weights on the lower excitations than those in the RHF orbitals from which they are derived, the effect is insignificant compared to that seen using UNOs.

There is a particular disparity between the two unrestricted bases in the intermediate stretching region, which was most challenging in the UHF basis. This difficulty, which arose from the requirement to highly populate a 6-fold excitation, is somewhat relieved by the UNOs. Taking the system with  $r = 4.2 a_0$  as an example, we find that the coefficient of that determinant is reduced by a factor of around 2.5 in favor of lower excitations. At the same time, the total sum of the coefficients,  $\sum_i |C_i|$ , reduces slightly from 6.72 in the UHF basis to 6.55 in the UNO. Correspondingly, an *i*-FCIQMC calculation in the UNO basis relaxes more rapidly than one in its corresponding UHF basis.

Allied to this effect is the fact that the Hamiltonian cast in the UNO basis provides many more paths between the reference state and its spin-flipped counterpart. Where in the UHF basis there were 150 coupling paths between  $|D_{0,L}\rangle$  and  $|D_{0,R}\rangle$  for the case  $r = 6.0 a_0$ , the UNO basis provides 1782, and this increased connection further ameliorates the sampling.

## 4. CONCLUSIONS

The flexibility afforded by the invariance of FCIQMC under orthogonal orbital rotation allows unrestricted orbitals to be used wherever they are advantageous. The use of such orbitals on the homonuclear diatomics leads to increasingly compact wave functions as the bonds are stretched, whereas the corresponding wave functions expressed in RHF orbitals become dense and thus more difficult to discretize in a walker representation. More generally, we have found that the precise choice of orbital basis can make a large difference in the sparsity of the ground-state eigenvector. Thus, for example, split-localized orbitals coming from a large CASSCF calculation do not lead to an efficient basis in the stretched limit of the  $N_2$  molecule and neither do the exact RNOs, whereas the exact UNOs do.

The UHF Hilbert space becomes nonergodic as the bond is stretched, and the total wave function may be written as the sum of two weakly coupled functions, residing in different

pockets of the space. We show that *i*-FCIQMC calculations initialized on the Hartree–Fock determinant provide excellent energies, albeit at the expense of spin purity. This is addressed by initializing the calculation on both the Hartree–Fock determinant and the dominant determinant of the other pocket, whereupon a spin-pure wave function is obtained which is still significantly more compact than the corresponding RHF expansion.

The most efficient basis appears to be the exact UNOs, which alleviate the ergodic problem while retaining the compactness of UHF expansions. These orbitals, therefore, present a promising avenue toward widening the scope of *i*-FCIQMC. To that end, schemes are now in development whereby they may be approximated without first having to solve the full problem in a less favorable basis.

## AUTHOR INFORMATION

### Corresponding Author

\*E-mail: asa10@cam.ac.uk.

### Notes

The authors declare no competing financial interest.

## ACKNOWLEDGMENTS

The authors acknowledge Trinity College, Cambridge, EPSRC, and the Cambridge Home and EU Scholarship scheme for funding. The calculations made use of the facilities of the Swiss National Supercomputing Centre (CSCS).

## REFERENCES

- (1) Coulson, C. A.; Fischer, I. *Philos. Mag.* **1949**, *40*, 386.
- (2) Knowles, P. J.; Handy, N. C. *Chem. Phys. Lett.* **1984**, *111*, 315.
- (3) Olsen, J.; Roos, B.; Jørgensen, P.; Jensen, H. J. *Chem. Phys.* **1988**, *89*, 2185.
- (4) Bendazzoli, G.; Evangelisti, S. J. *Chem. Phys.* **1993**, *98*, 3141.
- (5) Zarrabian, S.; Sarma, C.; Paldus, J. *Chem. Phys. Lett.* **1989**, *155*, 183.
- (6) Booth, G. H.; Thom, A. J. W.; Alavi, A. J. *Chem. Phys.* **2009**, *131*, 054106.
- (7) Cleland, D.; Booth, G. H.; Alavi, A. J. *Chem. Phys.* **2010**, *132*, 041103.
- (8) Feller, D.; Sordo, J. A. J. *Chem. Phys.* **2000**, *113*, 485.
- (9) Bak, K. L.; Jørgensen, P.; Olsen, J.; Helgaker, T.; Gauss, J. *Chem. Phys. Lett.* **2000**, *317*, 116.
- (10) Feller, D.; Peterson, K. A. J. *Chem. Phys.* **1998**, *108*, 154.
- (11) Peterson, K. A.; Wilson, A. K.; Woon, D. E.; Dunning, T. H., Jr. *Theor. Chim. Acta* **1997**, *97*, 251.
- (12) Filippi, C.; Umrigar, C. J. J. *Chem. Phys.* **1996**, *105*, 213.
- (13) Schmidt, M. W.; Lam, M. T. B.; Elbert, S. T.; Ruedenberg, K. *Theor. Chim. Acta* **1985**, *68*, 69.
- (14) Al-Saidi, W. A.; Zhang, S.; Krakauer, H. J. *Chem. Phys.* **2007**, *127*, 144101.
- (15) Purwanto, W.; Al-Saidi, W. A.; Krakauer, H.; Zhang, S. J. *Chem. Phys.* **2008**, *128*, 114309.
- (16) Purwanto, W.; Zhang, S.; Krakauer, H. J. *Chem. Phys.* **2009**, *130*, 094107.
- (17) Booth, G. H.; Cleland, D.; Thom, A. J. W.; Alavi, A. J. *Chem. Phys.* **2011**, *135*, 084104.
- (18) Cleland, D.; Booth, G. H.; Overy, C.; Alavi, A. J. *Chem. Theory Comput.* **2012**, *8*, 4138.
- (19) Booth, G. H.; Alavi, A. J. *Chem. Phys.* **2010**, *132*, 174104.
- (20) Cleland, D. M.; Booth, G. H.; Alavi, A. J. *Chem. Phys.* **2011**, *134*, 024112.
- (21) Booth, G. H.; Grüneis, A.; Kresse, G.; Alavi, A. *Nature* **2013**, *493*, 365.
- (22) Shepherd, J. J.; Booth, G. H.; Alavi, A. J. *Chem. Phys.* **2012**, *136*, 244101.
- (23) Hehre, W. J.; Stewart, R. F.; Pople, J. A. J. *Chem. Phys.* **1969**, *51*, 2657.
- (24) Werner, H.-J.; Knowles, P. J.; Knizia, G.; Manby, F. R.; Schütz, M.; Celani, P.; Korona, T.; Lindh, R.; Mitrushenkov, A.; Rauhut, G.; Shamasundar, K. R.; Adler, T. B.; Amos, R. D.; Bernhardsson, A.; Berning, A.; Cooper, D. L.; Deegan, M. J. O.; Dob-byn, A. J.; Eckert, F.; Goll, E.; Hampel, C.; Hesselmann, A.; Hetzer, G.; Hrenar, T.; Jansen, G.; Köppl, C.; Liu, Y.; Lloyd, A. W.; Mata, R. A.; May, A. J.; McNicholas, S. J.; Meyer, W.; Mura, M. E.; Nicklass, A.; O'Neill, D. P.; Palmieri, P.; Peng, D.; Pflüger, K.; Pitzer, R.; Reiher, M.; Shiozaki, T.; Stoll, H.; Stone, A. J.; Tarroni, R.; Thorsteins-son, T.; Wang, M. *MOLPROa* package of ab initio programs, version 2012.1; 2012; University College Cardiff Consultants Limited: Cardiff, U.K., 2012; <http://molpro.net>.
- (25) Bytautas, L.; Ivanic, J.; Ruedenberg, K. J. *Chem. Phys.* **2003**, *119*, 8217.
- (26) Pipek, J.; Mezey, P. G. J. *Chem. Phys.* **1989**, *90*, 4916.
- (27) Foster, J. M.; Boys, S. F. *Rev. Mod. Phys.* **1960**, *32*, 300.
- (28) Knowles, P. J.; Werner, H.-J. *Chem. Phys. Lett.* **1985**, *115*, 259.
- (29) Werner, H.-J.; Knowles, P. J. J. *Chem. Phys.* **1985**, *82*, 5053.
- (30) Krogh, J. W.; Olsen, J. *Chem. Phys. Lett.* **2001**, *344*, 578.
- (31) Laidig, W. D.; Saxe, P.; Bartlett, R. J. J. *Chem. Phys.* **1987**, *86*, 887.
- (32) Gwaltney, S. R.; Byrd, E. F. C.; Voorhis, T. V.; Head-Gordon, M. *Chem. Phys. Lett.* **2002**, *353*, 359.
- (33) Li, X.; Paldus, J. *Chem. Phys. Lett.* **1998**, *286*, 145.
- (34) Kucharski, S. A.; Watts, J. D.; Bartlett, R. J. *Chem. Phys. Lett.* **1999**, *302*, 295.
- (35) Larsen, H.; Olsen, J.; Jørgensen, P.; Christiansen, O. J. *Chem. Phys.* **2000**, *113*, 6677.
- (36) Dunning, T. H., Jr. J. *Chem. Phys.* **1989**, *90*, 1007.
- (37) Chan, G. K.-L.; Kállay, M.; Gauss, J. J. *Chem. Phys.* **2004**, *121*, 6110.
- (38) Shao, Y.; Fusti-Molnar, L.; Jung, Y.; Kussmann, J.; Ochsenfeld, C.; Brown, S. T.; Gilbert, A. T.; Slipchenko, L. V.; Levchenko, S. V.; O'Neill, D. P.; DiStasio, R. A.; Lochan, R. C.; Wang, T.; Beran, G. J.; Besley, N. A.; Herbert, J. M.; Yeh Lin, C.; Van Voorhis, T.; Hung Chien, S.; Sodt, A.; Steele, R. P.; Rassolov, V. A.; Maslen, P. E.; Korambath, P. P.; Adamson, R. D.; Austin, B.; Baker, J.; Byrd, E. F. C.; Dachselt, H.; Doerksen, R. J.; Dreuw, A.; Dunietz, B. D.; Dutoi, A. D.; Furlani, T. R.; Gwaltney, S. R.; Heyden, A.; Hirata, S.; Hsu, C.-P.; Kedziora, G.; Khalliulin, R. Z.; Klunzinger, P.; Lee, A. M.; Lee, M. S.; Liang, W.; Lotan, I.; Nair, N.; Peters, B.; Proynov, E. I.; Pieniazek, P. A.; Min Rhee, Y.; Ritchie, J.; Rosta, E.; David Sherrill, C.; Simmonett, A. C.; Subotnik, J. E.; Lee Woodcock, H.; Zhang, W.; Bell, A. T.; Chakraborty, A. K.; Chipman, D. M.; Keil, F. J.; Warshel, A.; Hehre, W. J.; Schaefer, H. F.; Kong, J.; Krylov, A. I.; Gill, P. M. W.; Head-Gordon, M. *Phys. Chem. Chem. Phys.* **2006**, *8*, 3172.
- (39) Flyvbjerg, H.; Petersen, H. G. J. *Chem. Phys.* **1989**, *91*, 461.
- (40) Huber, K. P.; Herzberg, G. *Molecular Spectra and Molecular Structure. IV. Constants of Diatomic Molecules*; Van Nostrand-Reinhold: Princeton, NJ, 1979.
- (41) Helgaker, T.; Jørgensen, P.; Olsen, J. *Molecular Electronic Structure Theory*; Wiley: New York, 2000; p 21.
- (42) Löwdin, P.-O. *Phys. Rev.* **1955**, *97*, 1474.
- (43) Booth, G. H.; Cleland, D. M.; Alavi, A.; Tew, D. J. *Chem. Phys.* **2012**, *137*, 1641.